The transverse laser induced thermoelectric voltages in step flow growth $(1-x)Pb(Mg_{1/3}Nb_{2/3})O_3$–$xPbTiO_3$ thin films*

Shang Jie(尚 杰)[a], Zhang Hui(张 辉)[a], Li Yong(李 勇)[a],
Cao Ming-Gang(曹明刚)[a], and Zhang Peng-Xiang(张鹏翔)[a)b)†]

[a] *Institute of Advanced Materials for Photoelectronics, Kunming University of Science and Technology, Kunming* 650051, *China*
[b] *MPI, FKF, Stuttgart D-*70569, *Germany*

(Received 30 November 2009; revised manuscript received 23 April 2010)

This paper reports that the transverse laser induced thermoelectric voltages (LITV) are observed for the first time in the step flow growth $(1-x)Pb(Mg_{1/3}Nb_{2/3})O_3$–$xPbTiO_3$ (PMN–PT, x = 0.20, 0.33, 0.50) thin films deposited on vicinal-cut strontium titanate single crystal substrates. Because lead magnesium niobate-lead titanate is a solid solution of lead magnesium niobate (PMN) and lead titanate (PT), there are two types of signals. One is wide with a time response of a microsecond, and the other superimposed with the wide signal is narrow with a time response of a nanosecond. The transverse LITV signals depend on the ratio of PMN to PT drastically. Under the irradiation of 28-ns pulsed KrF excimer laser with the 248-nm wavelength, the largest induced voltage is observed in the $0.50Pb(Mg_{1/3}Nb_{2/3})O_3$–0.50 $PbTiO_3$ films. Moreover, the effects of film thickness, substrates, and tilt angles of substrates are also investigated.

Keywords: laser induced thermoelectric voltage, $(1-x)Pb(Mg_{1/3}Nb_{2/3})O_3$–$xPbTiO_3$ films, anisotropic Seebeck effect

PACC: 7220P, 8630M, 4260K, 4255G

1. Introduction

Lead magnesium niobate ($Pb(Mg_{1/3}Nb_{2/3})O_3$, PMN) is a relaxor ferroelectric material[1−8] with high dielectric constant ($K \sim 20000$) and large electric-field-induced strain. Therefore, PMN is extensively used as capacitor and also as an electrostrictive actuator.[9−15] The PMN can form a solid solution, lead magnesium niobate–lead titanate (PMN–PT), with ferroelectric lead titanate ($PbTiO_3$, PT) which can enhance the dielectric properties of PMN. Single crystal of PMN–PT near the morphotropic phase boundary (MPB) has been reported to exhibit very high piezoelectric coefficients ($d_{33} > 2500$ pC/N) and extremely large piezoelectric strains ($> 1.7\%$). These values are significantly higher than those provided by the best lead zirconate titanate (PZT) based piezoceramics (600–700 pC/N and 0.17%).[16−18] So PMN–PT is a better substitute for PZT in many actuator and sensor applications.[19,20] Most of the present studies have focused on dielectric, piezoelectric and/or electromechanical properties, especially near the MPB region. Little work has been done on their potential applications.

In this paper, pure perovskite PMN–PT thin films were successfully deposited on vicinal-cut strontium titanate single crystal substrates by pulsed laser deposition (PLD). The result of x-ray diffraction (XRD) showed that the PMN–PT thin films were of a pure perovskite structure. The transverse LITV in PMN–PT thin films deposited on tilted strontium titanate single crystal substrates were observed for the first time.

2. Experimental procedure

To ensure the formation of a single perovskite phase, PMN–PT targets were synthesized using a two-

*Project supported by the National Natural Science Foundation of China (Grant No. 10274026).
†Corresponding author. E-mail: pxzhang@hotmail.com, sjkm06@yahoo.com.cn
© 2010 Chinese Physical Society and IOP Publishing Ltd

step method by the solid state reaction.

The heterostructures of PMN–PT thin films were prepared by PLD method using a KrF excimer laser (LPX300, Lambda Physik). The PLD method of thin film growth involves evaporation of a solid target in an ultra high vacuum chamber by means of short and high-energy laser pulses. The distance between the target and the substrate was kept at 45 mm. In a typical PLD process, a ceramic target is placed in a vacuum chamber. A pulsed laser beam ionizes the surface of the target, and the plasma condenses on a substrate.

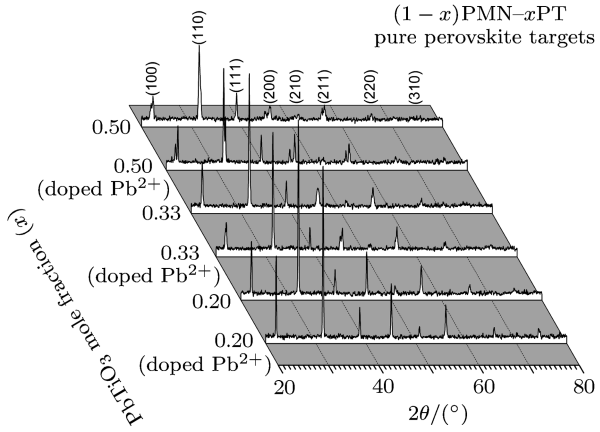


Fig. 1. XRD patterns of pure perovskite PMN–PT targets for the different ratios of PMN to PT.

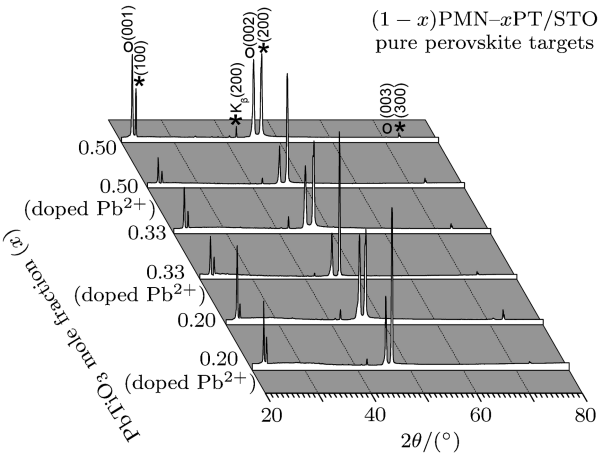


Fig. 2. XRD patterns of pure perovskite PMN–PT thin films for the different ratios of PMN to PT on $SrTiO_3$ along (001) orientation. (O) PMN–PT and (∗) $SrTiO_3$.

The structure of the PMN–PT targets and the thin films was characterized by XRD (BDX3200 Peking University) using $CuK_{\alpha 1}$ radiation (wavelength: 1.54056 Å, 1 Å=0.1 nm). The XRD patterns are shown in Figs. 1 and 2.

3. Results and discussion

Figure 3 shows a laser-induced voltage signal of PMN–PT thin film on vicinal-cut strontium titanate single crystal substrate, induced by the KrF excimer laser pulse with the 248-nm wavelength. As can be seen in Fig. 3, there are two signals. One is wide, and the other superimposed with the wide signal is a narrow one. The PMN–PT is solid solutions of PMN and PT. The PMN is a typical relaxor ferroelectric, but PT is a normal ferroelectric. For different ferroelectric, the coefficient of thermal conductivity is very different. However, response time of LITV signal is usually related to coefficient of thermal conductivity. That is why the LITV signals are composed of two signals with different response time.

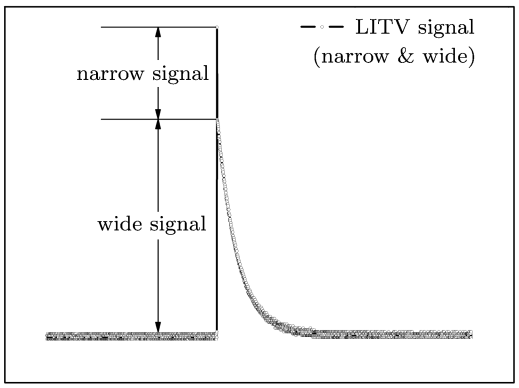


Fig. 3. A laser-induced voltage signal of PMN–PT thin film on tilted $SrTiO_3$ substrates along (001) orientation induced by the KrF excimer laser pulse with $\lambda = 248$ nm.

Figure 4 shows the LITV signals of the different PMN–PT thin films grown on 10° tilted strontium titanate single crystal substrates. It can be seen that the LITV signals are very different for the different ratios of PMN to PT. But, for the same PMN–PT thin films, there is a linear relation between the peak value voltages and incident laser energy. With the increase of x (x = 0.20, 0.33, 0.50), the peak value voltages also increase gradually.

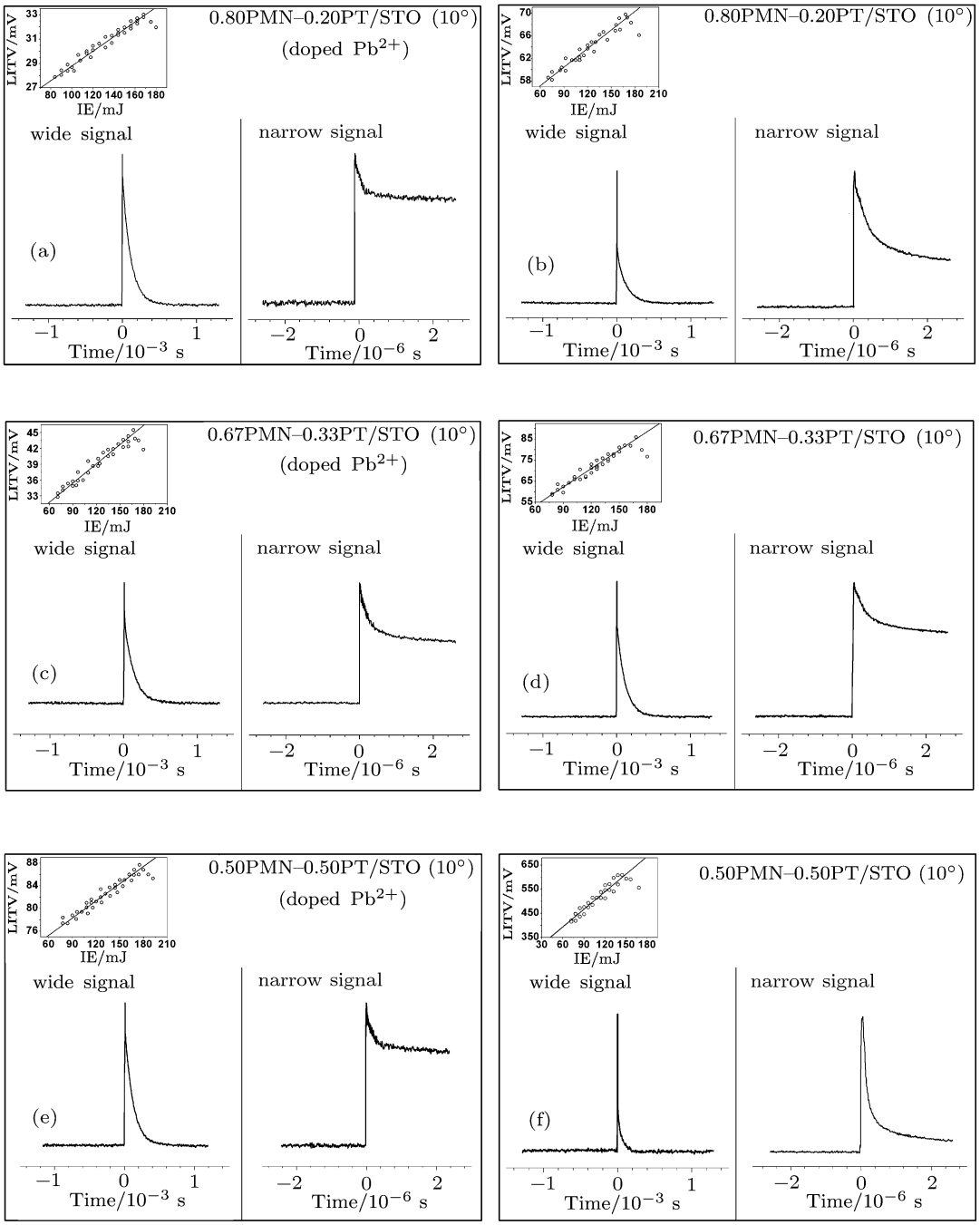


Fig. 4. Laser-induced voltage signals of the $(1-x)$PMN–xPT ($x = 0.20$, 0.33, 0.50) thin films on 10° tilted $SrTiO_3$ substrates along (001) orientation induced by the KrF excimer laser pulse with $\lambda = 248$ nm: (a) LITV signals of 0.80PMN–0.20PT doped 5 mol% Pb^{2+}; (b) LITV signals of 0.80PMN–0.20PT; (c) LITV signals of 0.67PMN–0.33PT doped 5 mol% Pb^{2+}; (d) LITV signals of 0.67PMN–0.33PT; (e) LITV signals of 0.50PMN–0.50PT doped 5 mol% Pb^{2+}; (f) LITV signals of 0.50PMN–0.50PT.

The comparison of the peak value voltages is shown in Fig. 5. However, the full widths at half maximum (FWHM) are almost constant except the one of 0.50PMN–0.50PT thin films. The comparison of the FWHM is shown in Fig. 6.

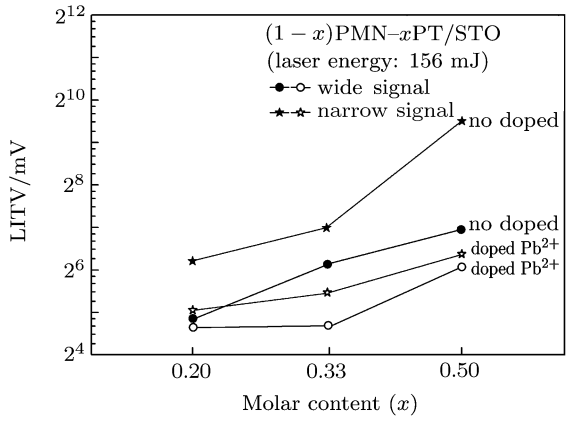


Fig. 5. The comparison of the peak value voltages for the $(1-x)$PMN–xPT ($x = 0.20, 0.33, 0.50$) thin films on 10° tilted $SrTiO_3$ substrates along (001) orientation induced by the KrF excimer laser pulse with $\lambda = 248$ nm.

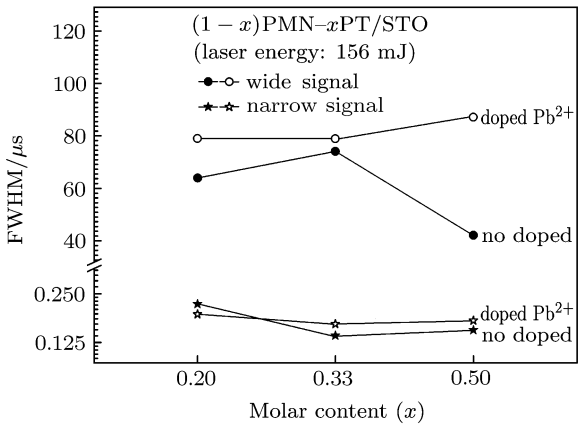


Fig. 6. The comparison of the FWHM for the $(1-x)$PMN–xPT ($x = 0.20, 0.33, 0.50$) thin films on 10° tilted $SrTiO_3$ substrates along (001) orientation induced by the KrF excimer laser pulse with $\lambda = 248$ nm.

Here, our interest is in the laser energy detection by using the LITV effect, thus we seek for the materials with higher peak value voltages and narrower FWHM. It can be seen that the 0.50PMN–0.50PT thin films are the best in all of the PMN–PT thin films through the comparison above.

Furthermore, the effects of film thickness, substrates, and tilt angles of substrates were also researched. It is shown in Figs. 7 and 8. We can easily see that the LITV signals have significant differences on the different substrates. But for the same substrate, the peak value voltages first increase and then decrease with the increase of the tilt angles of substrates and the film thickness.

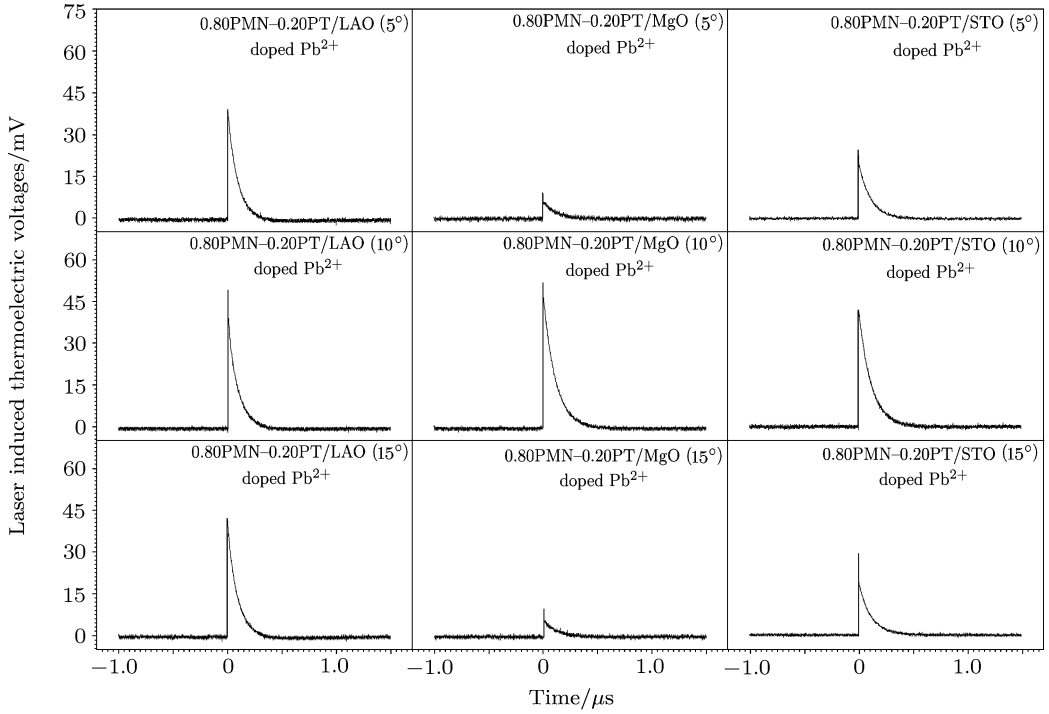


Fig. 7. The comparison of pure perovskite 0.80PMN–0.20PT (doped 5 mol% Pb^{2+}) thin films' LITV signals from three tilt angles grown on $LaAlO_3$, MgO and $SrTiO_3$ substrates respectively with the same conditions.

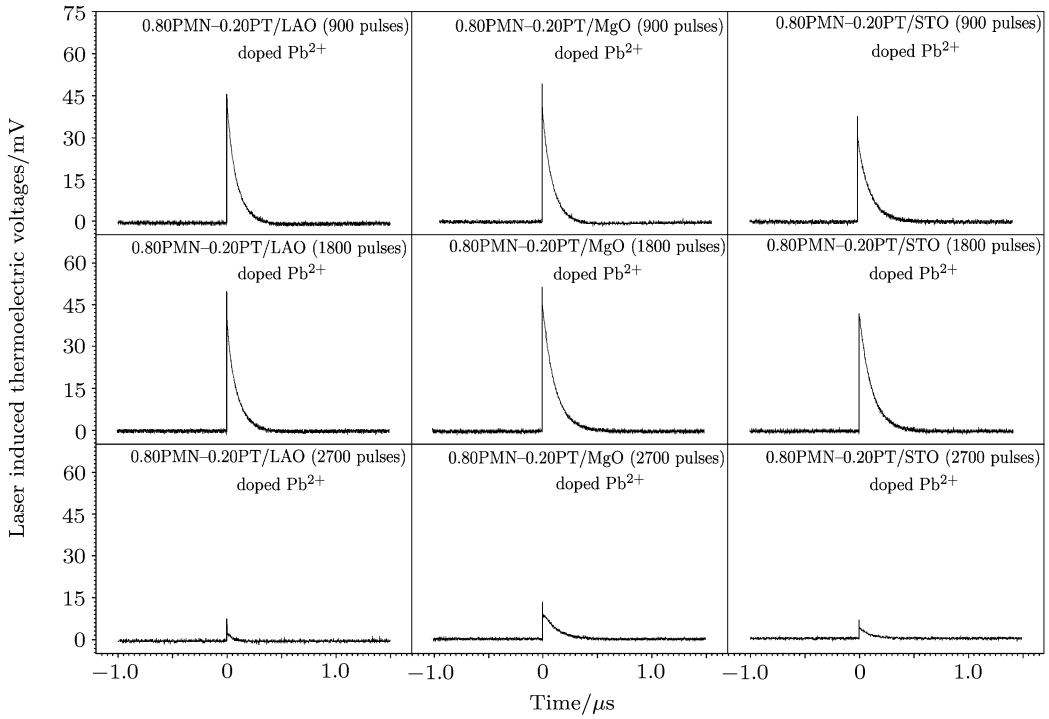


Fig. 8. The comparison of pure perovskite 0.80PMN–0.20PT (doped 5 mol% Pb^{2+}) thin films' LITV signals from three film thickness grown on $LaAlO_3$, MgO and $SrTiO_3$ substrates respectively with the same conditions.

According to the LITV formula (Eq. (1)) derived by Zhang *et al.*,[21] the film thickness has an optimum value, which is consistent with the experimental results. However, the signals should be increased with the increase of the tilt angles of substrates, which is inconsistent with the experimental results, mainly because the defects in the thin films increase with the increase of the tilt angles of substrates. The defects reduce the crystalline quality of the films. But the peak value is strongly related to the crystalline quality. Therefore, the signals become smaller, which is not incompatible with Eq. (1).

$$U(t) = \frac{\alpha_0 El \sin(2\alpha)}{4d\rho c_0\sqrt{\pi Dt}}(S_{\rm ab} - S_{\rm c}) \times (\mathrm{e}^{-\delta^2/4Dt} - \mathrm{e}^{-\mathrm{d}^2/4Dt}), \quad (1)$$

where α_0 is the laser absorption coefficient of film, E the laser energy density per pulse (for convenience, we also make E stand for laser energy per pulse), l is the illuminated length of film, α is the vicinal-cut angle, $S_{\rm ab} - S_{\rm c}$ is the Seebeck coefficient anisotropy, ρ is the mass density, c_0 is the specific heat, δ is the laser penetrating depth into the thin film material, D is the thermal diffusion constant, d is the film thickness.

4. Summary

The transverse LITV in the tilted PMN–PT thin films was observed for the first time. The LITV signals depend on the ratio of PMN to PT drastically. The maximum peak value voltage and minimum FWHM signal were found in the 0.50PMN–0.50PT thin films. Moreover, film thickness, substrates, and tilt angle of substrates also had an effect on the LITV signals. But they were all consistent with the LITV formula derived by Zhang *et al.*

References

[1] Zhou D, Lou L H, Wang F F, Jia Y M, Zhao X Y and Luo H S 2008 *Acta Phys. Sin.* **57** 4552 (in Chinese)

[2] Jayasingh E M, Prabhakaran K, Sooraj R, Durgaprasad C and Sharma S C 2009 *Ceramics International* **35** 591

[3] Smolenskii G A and Agranovskaya A I 1958 *Sov. Phys.*

Tech. Phys. (Engl. Transl.) **3** 1380

[4] Smolenskii G A and Agranovskaya A I 1959 *Sov. Phys. Solid State* **1** 1429

[5] Smolenskii G A, Isupov V A, Agranovskaya A I and Popov S N 1961 *Sov. Phys. Solid State* **2** 2584

[6] Krillov V V and Isupov V A 1973 *Ferroelectrics* **5** 3

[7] Cross L E 1987 *Ferroelectrics* **76** 241

[8] Cross L E 1994 *Relaxor Ferroelectrics: an Overview, Ferroelectrics* **151** 305

[9] Feng Z Y, Luo H S, Yin Z W, Guang H L and Ling N 2003 *Acta Phys. Sin.* **53** 3609 (in Chinese)

[10] Panda P K and Sahoo B 2005 *Materials Chemistry and Physics* **93** 231

[11] Swartz S L, Shrout T R, Schulze W A, Cross L E and Am J 1984 *Ceram. Soc.* **67** 311

[12] Nomura S and Uchino K 1982 *Ferroelectrics* **41** 117

[13] Uchino K and Am J 1986 *Ceram. Soc. Bull.* **65** 647

[14] Shrout T R, Halliyal A and Am J 1987 *Ceram. Soc. Bull.* **66** 704

[15] Chen J, Harmer M P and Am J 1990 *Ceram. Soc.* **73** 68

[16] Park S E and Shrout T R 1997 *J. Appl. Phys.* **82** 1804

[17] Shrout T R, Chang Z P, Kim N and Markgraf S 1990 *Ferroelectrics Lett. Sect.* **12** 63

[18] Ghasemifard M, Hosseini S M and Khorrami G H 2009 *Ceramics International* **35** 36

[19] Damjanovic D and Newnham R E 1992 *J. Intell. Mater. Syst. Struct.* **3** 190

[20] Uchino K 1986 *IEEE Trans.Ultrason., Ferroelectr. Freq. Control* **33** 806

[21] Zhang G Y, Zhang P X, Zheng H R, Zhang X Y, Gao D L, Zhang H, Pi L and Lee W K 2008 *Optics & Laser Technology* **40** 845